Technical Note

Validation of an In-Situ Material Qualification Method for PEM Fuel Cells Using Statistical Confidence Analysis

Denis Grün and Ulrich Misz *

Posted Date: 18 March 2026

doi: 10.20944/preprints202603.1419.v1

Keywords: proton exchange membrane fuel cell (PEMFC); balance of plant (BOP); in-situ material qualification; gas contamination; membrane electrode assembly (MEA) degradation; confidence intervals; t-test

 doi:10.20944/preprints202603.1419.v1

Technical Note

Validation of an In-Situ Material Qualification Method for PEM Fuel Cells Using Statistical Confidence Analysis

Denis Grün and Ulrich Misz *

The Hydrogen and Fuel Cell Center (ZBT GmbH), Carl-Benz-Strasse 201, 47057 Duisburg, Germany

* Correspondence: u.misz@zbt.de

Abstract

Due to high sensitivity of proton exchange membrane fuel cells (PEMFC) to feed gas contamination through balance of plant (BOP) materials, in-situ qualification plays a crucial role to secure performance, durability, and economic viability. To be able to deliver verified and accurate qualification results it is necessary to analyze the test method in detail and to perform repetitions on certain measurements. This work focuses on validation of an in-situ material qualification test method in terms of measuring precision on a previously developed test bench and statistical significance of collected data. As a statistical approach t-test was used to calculate confidence intervals based on a sample size of 15 reference measurements with the same parameters and setup but variable membrane electrode assemblies (MEA). The results show substantial reduction of confidence intervals with growing measurement's sample size clearly quantifying accuracy of the analyzed methodology. The precision of the test method, as indicated by the calculated confidence intervals of irreversible voltage loss is approx. 1.21 mV, corresponding to a relative deviation of about 0.17% with respect to the calculated mean value across all steady-state phases (SSPs). This approach also provides an insight into the natural degradation behavior of the tested MEAs. The calculated effects can serve as a basis for design of experiments (DOE) in future test series.

Keywords: proton exchange membrane fuel cell (PEMFC); balance of plant (BOP); in-situ material qualification; gas contamination; membrane electrode assembly (MEA) degradation; confidence intervals; t-test

1. Introduction

Internal and external contamination of proton exchange membrane fuel cells (PEMFC) caused by catalyst poisoning through desorbed very volatile and volatile organic compounds (VVOCs/VOCs) from integrated balance of plant (BOP) components in the system (e.g., sealings, hoses, connectors), impurities in the atmospheric air or hydrogen aging is still rarely researched subject with a limited number of publications [1–6]. Besides the degradation aspect, which has an immense effect on the performance and durability, cost reduction is also necessary through the substitution of expensive materials for peripheral parts to facilitate the roll-out on the market for fuel cell technologies [7]. To analyze the direct link between desorbed emissions and reduction of electrochemical active area of the membrane electrode assembly (MEA), it is inevitable to focus on in-situ test method with a fuel cell coupling. National Renewable Energy Laboratory (NREL) in cooperation with US universities has developed a test method to bring contaminants from assembly aids into a liquid phase using leaching and then introduce leachate to a performing fuel cell through an infusion directly into a gas feed stream [7–9]. Subsequently, the same approach was used to qualify polythalamide leachate from structural material [10]. Furthermore, the leaching approach was applied to quantify potential contaminant concentration in leachate from styrene-butadiene rubber (SBR) and neoprene via gas chromatography-mass spectrometry (GCMS) and Fourier transform

 doi:10.20944/preprints202603.1419.v1

infrared attenuated total reflectance (FTIR-ATR) [11]. Also, a slightly different concept of a cationic contaminants infusion was introduced with a separate air gas feed stream through the nebulizer [12]. As an extension to the quantification of extracted solutions, electrochemical characterization such as cyclic voltammetry has been performed on 3-electrode ex-situ system to evaluate possible Pt catalyst poisoning due to leaching contaminants [13].

By producing aerosol with help of a nozzle, it is possible to analyze voltage behavior of the cell in presence of ions and trace particles from leachate, which can be brought into the system externally e.g., through the air feed stream [14]. Gaseous emissions with high vapor pressure and low boiling point such as some of VVOCs and VOCs, released due to a thermal activation, occur internally from integrated polymer components in the system [15]. Accordingly, the general motivation for our in-situ material qualification method arises from the recognition of this fact. The in-situ examination of thermally activated desorption in gaseous phase of BOP materials, in particular ethylene-propylene diene monomer (EPDM) and fluoroelastomer-based materials (FKM), using eight parallel operated PEMFCs, was carried out to observe the degradation effect and to determine a potential voltage loss [1]. The experimental setup of the study consists of eight separately operating PEMFCs sharing a common air feed inlet. The air stream passes through a heated aluminum sample holder, which can be bypassed using a directional control valve to enable reference measurements. The sample holder accommodates various materials that release gaseous emissions upon thermal activation. As the air feed passes through the holder, it transports these emissions into the fuel cells, where the resulting voltage response is monitored [16,17]. This approach may offer advantages when analyzing the voltage behavior of individual cells supplied by a common gas inlet, particularly with respect to emission distribution, while investigating one material at a time. However, if the comparability between the cells is not verified, evaluating different material across multiple single cells becomes challenging and may introduce uncertainties. In contrast, applying a single-cell setup enables clearer interpretation of results, requiring less technical complexity while improving reliability. It is also noted that the referenced study includes a limited number of repetitions (n = 2 per material), which restricts the statistical validity of the findings. Therefore, our research addresses these limitations by applying a single-cell approach and systematically repeating experiments to validate the methodology, thereby improving reproducibility and ensuring methodological rigor.

2. Materials and Methods

For the in-situ qualification of BOP materials, PEMFC from balticFuelCells® with a 25 cm² electrochemical active area is used. In addition, 15 µm thick membranes (240 µm thick gas diffusion layers) with a platinum loading of 0.4 mg/cm² on both the anode and cathode sides are employed. The standard bipolar plates from the manufacturer are replaced by graphite-based plates developed at Zentrum für BrennstoffzellenTechnik GmbH (ZBT), which feature a significantly finer flow field for improved gas distribution. An emission chamber has been developed for accommodation of samples in a reasonable way to maximize gas exposed material surface. It enables the positioning of tensile bars (DIN EN ISO 527-2 type 1A), as well as auxiliary assembly materials e.g., liquids or non-Newtonian fluids, using a custom-designed sample holder (Figure 1).

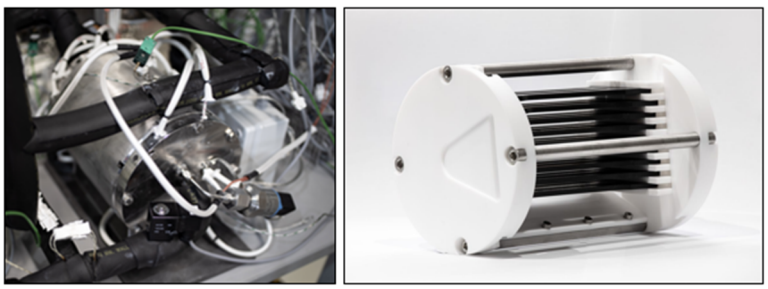

(**a**) (**b**)

 doi:10.20944/preprints202603.1419.v1

Figure 1. (a) Emission chamber integrated in the test rig; (b) Sample holder loaded with type 1A specimens (black).

The emission chamber can be heated up to 120 °C to expose the materials to a thermal stress and to stimulate the desorption of VVOCs/VOCs. Furthermore, a bypass of the emission chamber is integrated into the test bench, which allows performing of regeneration cycles by supplying fresh educt gas (hydrogen or air, depending on the placement of the chamber) after potential contamination of the MEA. The test fuel cell operates with humidified reactant gases (hydrogen and air). The gas flow rates are controlled via Alicat mass flow controllers and subsequently mixed with wet vapor from direct evaporators in a mixing chamber. Water injection dosing for the evaporators is managed via Bronkhorst liquid flow controllers and is linked to the National Instruments® compact data acquisition device (cDAQ) for precise humidity regulation of both gas feeds. Operating parameters include a pressure of 2 bar(a) on both the anode and cathode sides, 80 °C cell temperature, and 90 °C temperature in the emission chamber. Relative humidity is set to 85% in the anode and 69% in the cathode line through all steady state phases (SSP). The emission chamber was integrated in the anode gas feed in all further executed measurements. The humidity level in the chamber was lower (approx. 57%) as in the gas line due to the higher temperature in comparison to the test cell. Hydrogen with a purity grade of 5.0 (≥ 99.999%) was used in all experiments. The setup as well as schematic piping and instrumentation diagram (P&ID) of the test bench are shown in Figure 2. Deionized water is vaporized in the pre-humidifier and mixed with dry hydrogen in the mixing chamber. The humidified hydrogen then passes through the heated emission chamber containing the material samples, transporting potentially desorbed species directly to the anode side of the fuel cell.

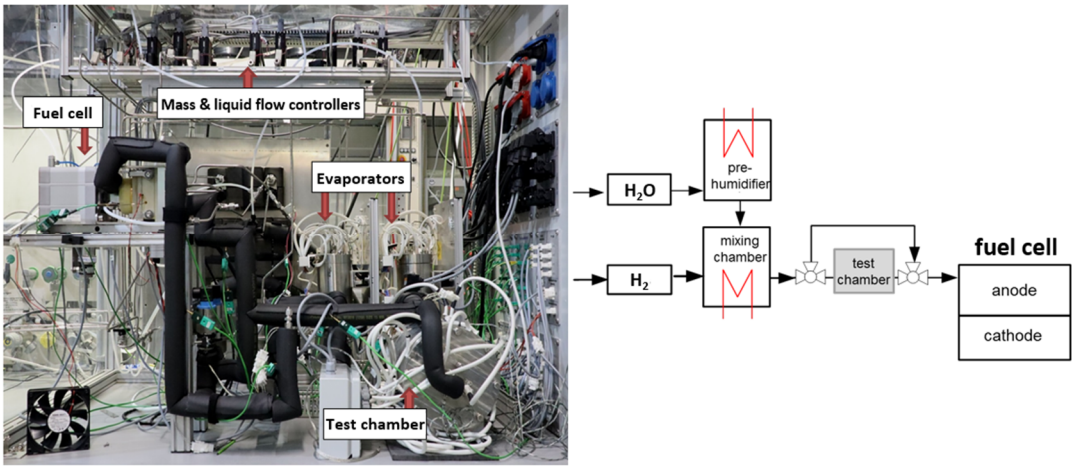

(**a**) (**b**)

Figure 2. (a) The setup of the test rig with the most relevant components shown; (b) Schematic P&ID of the anode gas feed line with the emission chamber.

The test procedure for material measurements includes a reference measurement (see Figure 3-a) with an empty sample holder, consisting of polytetrafluoroethylene (PTFE) and stainless steel (SS 316), as well as a sample measurement (Figure 3-b) with the holder loaded with specimens based on shown test protocol (Figure 3-c).

 doi:10.20944/preprints202603.1419.v1

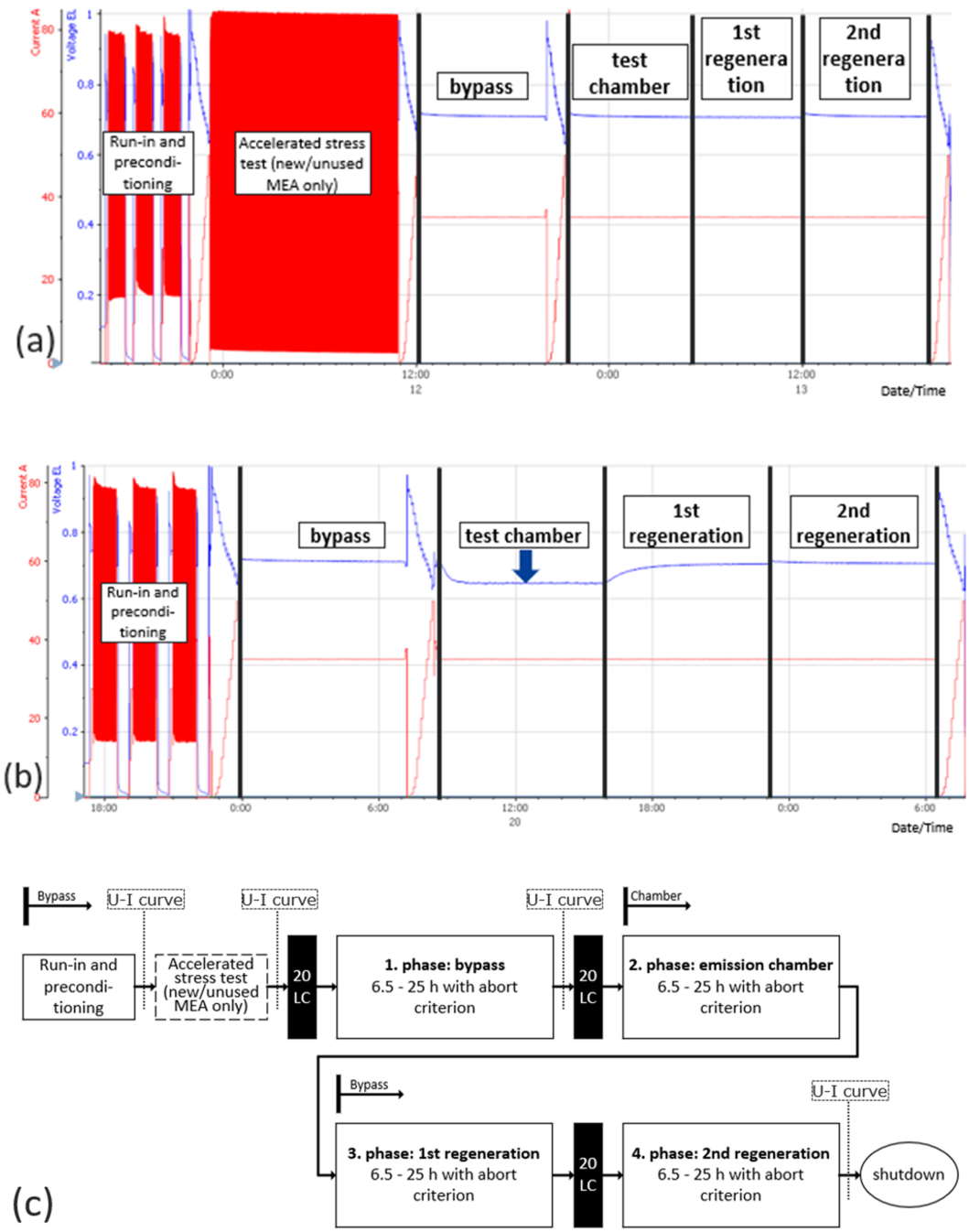

Figure 3. (a) Raw current and voltage data profiles of a reference measurement with new/unused MEA (voltage [V] in blue, current [A] in red); (b) Raw current and voltage data profiles of a sample measurement with a reused MEA (voltage [V] in blue, current [A] in red); (c) Schematic test protocol with SSPs.

The influence of the emitted substances on cell performance is evaluated based on the variable cell voltage and constant current. Figure 3-b presents an exemplary voltage decrease in the test chamber phase relative to the reference measurement (Figure 3-a). The test protocol (Figure 3-c) comprises beginning of life (BOL) sequence with three loops of potential cycling from 0.3 to 0.8 V and cool-down intervals between the loops. Following this, the first polarization curve is performed. Thereafter an accelerated stress test (AST) with high frequent potential cycling from 0.25 to 0.9 V is executed (only when using a new MEA). Finally, the second polarization curve is performed. Next, four SSPs with constant current density of 1.4 A/cm² and non-stoichiometric cell operation with 2.5 Nl/min air and 0.5 Nl/min hydrogen are imminent. The first SSP represents beginning of test (BOT). In this stage, 20 cycles of critical voltage alternation from 0.2 to 0.9 V are applied to the test cell to

 doi:10.20944/preprints202603.1419.v1

activate the catalyst and then the bypass measurement is executed to determine the actual performance of the MEA, which is followed by the third polarization curve. Before the test chamber phase (the second SSP), 20 critical potential cycles are performed again. The bypass line is closed and one of the reactant gases is directed through the chamber, transporting any potential contaminants desorbed from the materials to the test cell. The self-induced (SI) regeneration phase follows (the third SSP), using fresh gas via the bypass line while the emission chamber is shut. In the last SSP, 20 critical potential cycles are conducted, followed by alternate critical voltage (ACV) regeneration in the bypass. As an end of test (EOT), the fourth polarization curve is carried out. Each of the described SSPs lasts a minimum of 6.5 hours, and depending on the measured voltage drop, each phase may last up to 25 hours, in accordance with a termination criterion of 2 mV voltage loss within the last 30 minutes of a given phase. As long as no convergence in the voltage behavior is achieved, the operation time of a SSP will be automatically extended.

For the statistical analysis, a parametric approach based on two-sample Welch's t-test with unequal variances was applied using α (t) of 95% probability that the estimated mean of each sample will lay in the calculated confidence interval. To assess whether the null hypothesis (no significant difference) could be rejected, the condition $p < \alpha$ ($|t| > t_{crit}$) was used, with calculated two-sided p-value (interpreted as probability) and defined $\alpha = 0.05$ (significance level or cutoff threshold value, representing a 5% risk of falsely detecting a difference). Normality of each sample was examined using the Shapiro-Wilk test. To evaluate whether the null hypothesis (the data are normally distributed) could be retained, the condition $p > \alpha$ was used, with calculated p and defined $\alpha = 0.001$ (0.1% risk of falsely rejecting normality). Moreover the W values (test statistics) have been compared to ensure a normal distribution (criterion: $W_{calc} > W_{p,\ crit}$) [18]. All calculations were performed manually in Microsoft 365 Excel using the built-in Analysis-ToolPak. For validation and comparison, results were cross-checked using the 'Statistics Kingdom' web application [19].

3. Results

All 15 reference measurements have been performed with different MEAs but with the same handling, under the same operating conditions and unchanged test bench setup to ensure minimum variability. Six data extraction points (groups) have been defined:

- voltage in the beginning of the bypass U_{BB} (reference dataset for the t-test),
- voltage in the end of the bypass U_{BE},
- voltage in the beginning of the emission chamber U_{CB},
- voltage in the end of the emission chamber U_{CE},
- voltage in the beginning of the regeneration (SI & ACV) U_{RB},
- voltage in the end of the regeneration (SI & ACV) U_{RE},

depending on the SSP of each measurement for further analysis. Two datasets have been calculated:

- reversible voltage U_{Rev},

from the voltage difference between the end of the regeneration and the end of the emission chamber (U_{RE} - U_{CE}) and

- irreversible voltage U_{Irrev},

from the voltage difference between the end of the regeneration and the end of the bypass (U_{RE} - U_{BE}). With U_{Irrev} it is possible to quantify natural degradation of MEA and use it as a MEA exchange indicator for future material measurements after less reversible contaminations with bigger voltage drop in the emission chamber SSP. Positive values for U_{Rev} mean that voltage has been gained through the recovery phases. Negative values for U_{Irrev} mean that voltage has been lost during a whole measurement. In the next step normal distribution of each sample has been proven by means of Shapiro–Wilk test (Table 1).

 doi:10.20944/preprints202603.1419.v1

Table 1. Experimentally obtained and calculated data from the reference measurements. All voltages are measured in mV.

Obtained data								
MEA No.\Group	U_{BB}	U_{BE}	U_{CB}	U_{CE}	U_{RB}	U_{RE}	U_{Rev}	U_{Irrev}
MEA1	709.98	699.75	704.35	696.14	695.38	698.80	2.66	-0.95
MEA2	699.56	692.39	695.09	688.64	688.05	692.16	3.52	-0.23
MEA3	700.35	693.15	696.04	690.29	689.96	693.21	2.93	0.07
MEA4	699.52	691.83	695.81	689.01	688.48	691.80	2.79	-0.03
MEA5	693.18	684.90	687.13	679.74	678.42	684.44	4.70	-0.46
MEA6	697.95	690.39	688.61	684.77	682.60	689.83	5.06	-0.56
MEA7	694.40	687.92	686.90	683.35	681.61	687.79	4.44	-0.13
MEA8	710.40	701.33	704.82	699.75	699.16	700.90	1.15	-0.43
MEA9	699.36	692.06	693.57	687.69	686.48	691.01	3.32	-1.05
MEA10	695.28	688.45	690.98	683.22	682.83	687.99	4.77	-0.46
MEA11	710.34	700.84	706.29	698.08	697.85	700.28	2.20	-0.56
MEA12	704.06	699.29	703.89	697.16	698.11	699.62	2.46	0.33
MEA13	697.45	693.34	699.69	692.46	692.46	695.71	3.25	2.37
MEA14	702.19	697.58	703.57	697.39	697.26	699.65	2.27	2.07
MEA15	698.37	693.48	700.25	693.31	693.87	695.45	2.14	1.97
Calculated data								
Parameter\Group	U_{BB}	U_{BE}	U_{CB}	U_{CE}	U_{RB}	U_{RE}	U_{Rev}	U_{Irrev}
S-W, W_{calc}	0.891	0.944	0.922	0.952	0.937	0.940	0.945	0.799
S-W, $W_{p,\,crit}$	0.754	0.754	0.754	0.754	0.754	0.754	0.754	0.754
Probability p	0.069	0.431	0.203	0.551	0.345	0.383	0.454	0.004
Significance level α (S-W)	0.001	0.001	0.001	0.001	0.001	0.001	0.001	0.001
Mean value	700.82	693.78	697.13	690.73	690.17	693.91	3.18	0.13
Sample size	15	15	15	15	15	15	15	15
Standard deviation	5.61	5.00	6.73	6.23	6.78	5.21	1.14	1.10
Variance [mV²]	31.47	25.00	45.29	38.81	45.97	27.14	1.30	1.21
Significance level α (t)	0.05	0.05	0.05	0.05	0.05	0.05	0.05	0.05
Degrees of freedom	Ref.	28	27	28	27	28	15	15
Two-sided p-value	Ref.	0.63	0.76	0.97	0.77	0.97	0.67	0.64
$\lvert t \rvert$	Ref.	0.49	0.31	0.04	0.29	0.04	0.44	0.47
t_{crit}	Ref.	2.05	2.05	2.05	2.05	2.05	2.13	2.13
Lower bound confidence	Ref.	691.14	693.57	687.44	686.58	691.15	2.55	-0.48
Upper bound confidence	Ref.	696.42	700.70	694.03	693.76	696.66	3.80	0.73

Subsequently, Welch's two-sample t-test was performed, and each sample was compared with the reference dataset U_{BB}. Under previously described conditions, no statistically significant differences were observed between the datasets, as expected for repeated reference measurements. Also, the confidence intervals for each sample have been calculated, which are represented via confidence bounds for more detailed understanding of the measuring precision (see Figure A1 and Figure A2). To provide a proof that the introduced in-situ qualification method also applicable for material measurements, three different materials have been tested on three randomly picked MEAs directly after execution of the reference measurements. The material measurements have been also performed with the previously introduced test protocol and the same setup. 15 samples (DIN EN ISO 527-2 type 1A) of Neoflon RP5000 AS have been tested on the MEA4, as well as Ultramid A3EG7EQ on the MEA6 and Vestamid E62-S3 NC on the MEA9 (Figure 4). Variations in sensor cell response to emissions from the tested materials indicate that the method is effective. The voltage on the diagram is presented in % and 100% correlates to the mean value of the first 100 data points of the bypass phase, which is 698.81 mV. Before the first, second and fourth SSP, critical potential cycling is applied,

 doi:10.20944/preprints202603.1419.v1

resulting in a decreasing voltage gradient during the initial hours of operation. The operating times of each SSP variate due to the previously described abort criterion.

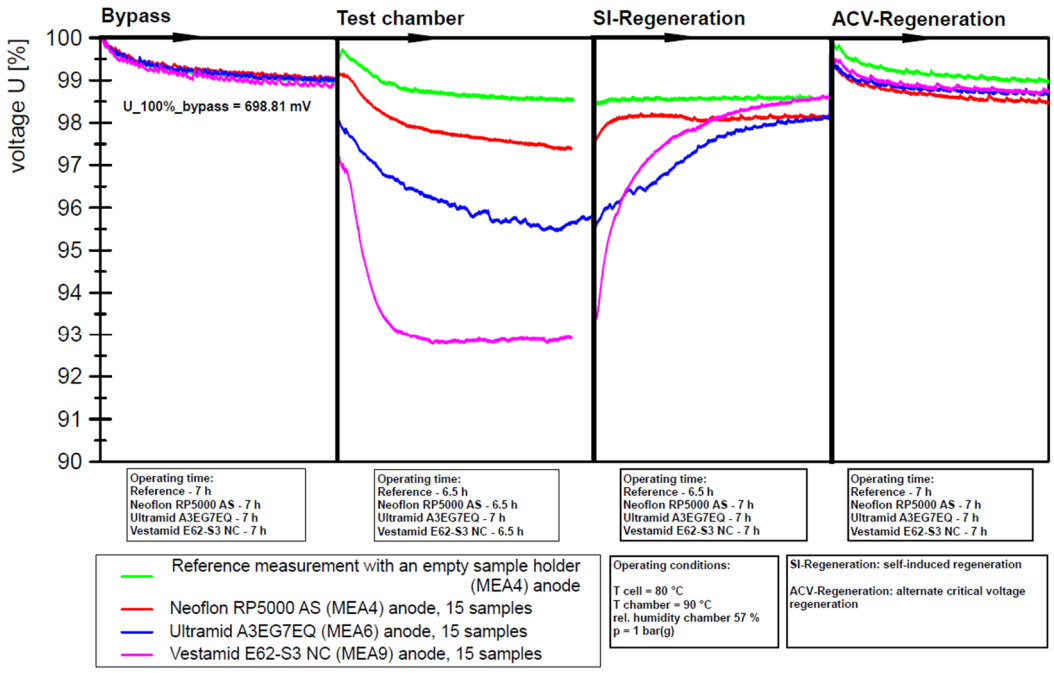

Figure 4. Visualized processed data of the three material measurements and a reference measurement.

The discontinuities in the plots are intentional and serve to enhance visualization and enable direct comparison of each SSP across the executed experiments. To improve clarity of the presented results, the data extraction points are summarized in Table 2.

Table 2. Experimentally obtained data from the material measurements. All voltages are measured in mV.

MEA No.\Group	U_{BB}	U_{BE}	U_{CB}	U_{CE}	U_{RB}	U_{RE}	U_{Rev}	U_{Irrev}
MEA4	703.30	695.97	697.78	684.70	685.09	692.03	7.33	-3.94
MEA6	702.94	695.45	690.22	671.13	671.36	693.08	21.96	-2.37
MEA9	710.96	702.61	691.14	659.49	663.01	700.87	41.38	-1.74

4. Discussion

Despite the use of different MEAs, the test results show a high level of consistency across measurements. The narrow confidence intervals observed indicate minimal variation between individual datasets, suggesting that the influence of MEA variability is negligible within the applied testing conditions. The confidence interval associated with the irreversible voltage loss is 1.21 mV, corresponding to a relative deviation of about 0.17% with respect to the mean cell voltage of approx. 694.42 mV across all SSPs, indicating that the contribution of natural degradation effect, during the relatively short testing period, is minimal. The high degree of reproducibility supports the robustness and precision of the measurement approach. Consequently, the results suggest that the developed in-situ qualification method may serve as a suitable tool for assessing the impact of material emissions on fuel cell performance, although these measurements were conducted without repetitions. The material screening revealed distinct differences in voltage response among the tested polymers during the emission chamber SSP, reaching values of up to approximately 41 mV (≈ 6%). Neoflon exhibited the best performance, showing an approx. voltage decrease of 1.5%. Ultramid demonstrated moderate behavior with a voltage reduction of about 3%, while Vestamid showed the most pronounced effect, reaching a voltage loss of approx. 6%. Notably, all tested materials showed strong reversibility already in the subsequent SI regeneration SSP. After the ACV regeneration SSP,

 doi:10.20944/preprints202603.1419.v1

all material curves returned to approximately the same voltage level, just below the reference curve, indicating quite successful recovery. These materials indicate a material-dependent impact on fuel cell performance under the applied test conditions, which should be analyzed in greater depth.

5. Conclusions

The statistical validation of the presented in-situ material qualification method demonstrates high measurement precision and reproducibility. The evaluation also provides insight into the natural degradation behavior of the tested MEAs. Although the observed irreversible voltage losses were small within investigated timeframe, further measurements are required to better characterize intrinsic degradation and to clearly separate it from contamination-induced effects. Methods such as polarization curve analysis, cyclic voltammetry and electrochemical impedance spectroscopy could provide valuable additional and deeper understanding. Material-specific voltage responses were observed, demonstrating the general applicability of the method. However, these measurements were conducted with a sample size of n = 1 per material and therefore lack statistical validity. Future work will include repeated measurements of identical materials, randomization of test sequences, and structured grouping of experiments. The executed experiments establish a foundation for subsequent DOE-based test planning, where statistical power analysis will be used to define appropriate repetition numbers and ensure statistically robust conclusions.

Author Contributions: Conceptualization, methodology, validation, formal analysis, investigation, data curation, writing—original draft preparation, visualization, D. Grün; writing—review and editing, project administration, U. Misz. All authors have read and agreed to the published version of the manuscript.

Funding: This research was funded by Bundesministerium für Wirtschaft und Energie, grant number 03ETB001C and the APC was covered by ZBT.

Data Availability Statement: All data generated or analyzed during this study are included in this article.

Acknowledgments: During the preparation of this manuscript, the authors used ChatGPT-5 for the purposes of language improvement. The authors have reviewed and edited the output and take full responsibility for the content of this publication.

Conflicts of Interest: The authors declare no conflicts of interest. The funders had no role in the design of the study; in the collection, analyses, or interpretation of data; in the writing of the manuscript; or in the decision to publish the results.

Abbreviations

The following abbreviations are used in this manuscript:

PEMFC	Proton exchange membrane fuel cell
BOP	Balance of plant
DOE	Design of experiments
MEA	Membrane electrode assembly
VVOCs	Very volatile organic compounds
VOCs	Volatile organic compounds
NREL	National renewable energy laboratory
SBR	Styrene-butadiene rubber
GCMS	Gas chromatography-mass spectrometry
FTIR-ATR	Fourier transform infrared attenuated total reflectance
EPDM	Ethylene-propylene diene monomer
FKM	Fluoroelastomer-based materials
ZBT	Zentrum für BrennstoffzellenTechnik GmbH
cDAQ	Compact data acquisition device
SSP	Steady state phase
P&ID	Piping and instrumentation diagram

 doi:10.20944/preprints202603.1419.v1

PTFE	Polytetrafluoroethylene
SS 316	Stainless steel 316 (1.4401)
BOL	Beginning of life
AST	Accelerated stress test
BOT	Beginning of test
SI	Self-induced
ACV	Alternate critical voltage
EOT	End of test

Appendix A

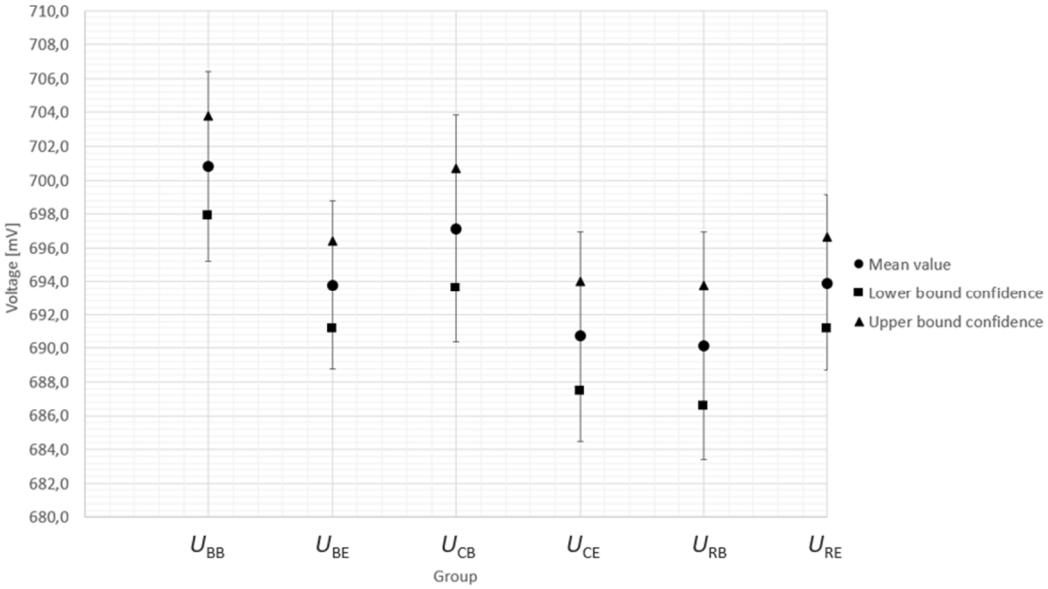

Figure A1. Visualized confidence intervals of the test groups with standard deviation error bars of the mean value.

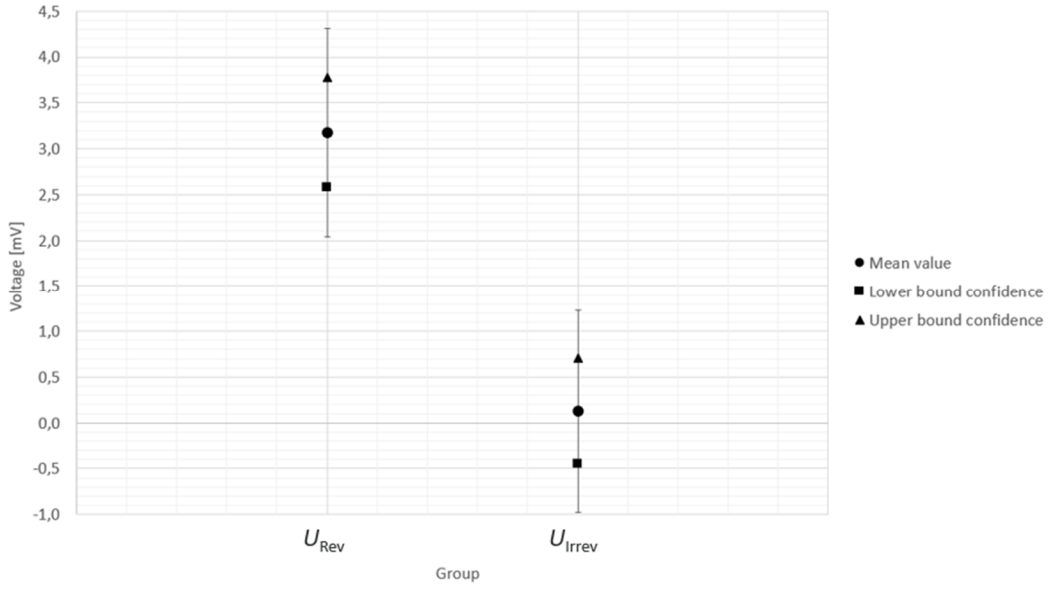

Figure A2. Visualized confidence intervals of the test groups with standard deviation error bars of the mean value (continued).

 doi:10.20944/preprints202603.1419.v1

References

1. Ali, F. S.; Daniel, L.; Heikkinen, N.; Ihonen, J.; Rautanen, M. Influence of contaminants on PEMFC performance – a multisinglecell approach. Next Research 2025 10.1016/j.nexres.2025.100209; 2(2):100209.
2. Moore, J. M.; Adcock, P. L.; Lakeman, J. B.; Mepsted, G. O. The effects of battlefield contaminants on PEMFC performance. Journal of Power Sources 85 2000 254–260 1999.
3. Morsbach, S.; Giersch, D.; Zhang, K. A. I.; Schüßling, A.; Weberskirch, D.; Börger, A. Hydrogen Compatibility of Polymers for Fuel Cell Vehicles. Energy Tech 2022 10.1002/ente.202200018; 10(9).
4. Mehrabadi, B. A. T.; Dinh, H. N.; Bender, G.; Weidner, J. W. Effect of System Contaminants on the Performance of a Proton Exchange Membrane Fuel Cell. J. Electrochem. Soc. 2016 10.1149/2.0761614jes; 163(14):F1527-F1534.
5. Misz, U.; Acker, K. Collaborative Project: VALIDATE. Research on validation methods for analyzing the influence of fluid path materials and stack/system components on fuel cell stack degradation. Subproject: In-situ analyses and identification of suitable materials.; Project report; 2020 [cited 2025 Dec 23]. Available from: URL: https://doi.org/10.2314/KXP:1809096561.
6. Finkenwirth, O.; Farajallah, H.; Frettlöh, V.; Frank, M.; Gärtner, L.; Runge, M. et al. Collaborative project: FaeBS. Functional design and experimental validation of an innovative fuel cell system.; Project report; 2024 [cited 2025 Dec 23]. Available from: URL: https://doi.org/10.2314/KXP:1929238800.
7. Opu, M.; Bender, G.; Macomber, C. S.; van Zee, J. W.; Dinh, H. N. Understanding the Effects of PEMFC Contamination from Balance of Plant Assembly Aids Materials: In Situ Studies. J. Electrochem. Soc. 2015 10.1149/2.0411509jes; 162(9):F1011-F1019.
8. Dinh, H. N.; Macomber, C.; Wang, H.; Bender, G.; O'Neill, K.; Pivovar, B. (V.B.1) Effect of System Contaminants on PEMFC Performance and Durability -: DOE Hydrogen and Fuel Cells Program FY 2012 Annual Progress Report; 2012.
9. Dinh, H. N.; Bender, G.; Macomber, C.; Wang, H. (V.E.3) Effect of System Contaminants on PEMFC Performance and Durability: Fiscal year progress report 2015.
10. Carey, C. T. Effect of Polythalamide Material Leachate on Platinum-alloy Polymer Electrolyte Membrane Performance [Office of Science, Science Undergraduate Laboratory Internship Program]. Columbia, SC: University of South Carolina; 2016.
11. Macomber, C. S.; Wang, H.; O'Neill, K.; Coombs, S.; Bender, G.; Pivovar, B. et al. Characterizing Polymeric Leachants for Potential System Contaminants of Fuel Cells. ECS Trans. 2010 10.1149/1.3484653; 33(1):1637–43.
12. Qi, J.; Wang, X.; Ozdemir, M. O.; Uddin, M. A.; Bonville, L.; Pasaogullari, U. et al. Effect of cationic contaminants on polymer electrolyte fuel cell performance. Journal of Power Sources 2015 10.1016/j.jpowsour.2015.03.142; 286:18–24.
13. Wang, H.; Macomber, C.; Dinh, H. N. Evaluation of PEMFC System Contaminants on the Performance of Pt Catalyst via Cyclic Voltammetry: Preprint.
14. Li, H.; Zhang, S.; Qian, W.; Yu, Y.; Yuan, X.; Wang, H. et al. Impacts of operating conditions on the effects of chloride contamination on PEM fuel cell performance and durability. Journal of Power Sources 2012 10.1016/j.jpowsour.2012.07.003; 218:375–82.
15. Moll, S. Study of the impact of thermal-oxidative exposure on the emission characteristics of ABS and PP and the correlation with material aging [PhD dissertation]. Erlangen-Nürnberg: Friedrich-Alexander University; 2017.
16. Auvinen, S.; Tingelöf, T.; Ihonen, J. K.; Siivinen, J.; Johansson, M. Stainless Steel In-situ Corrosion Testing in a PEFC Multisinglecell. ECS Trans. 2009 10.1149/1.3210737; 25(1):1811–21.
17. Auvinen, S.; Tingelöf, T.; Ihonen, J. K.; Siivinen, J.; Johansson, M. Cost Effective In-Situ Characterization of Coatings for PEFC Bipolar Plates Demonstrated with PVD Deposited CrN. J. Electrochem. Soc. 2011 10.1149/1.3562215; 158(5):B550.

 doi:10.20944/preprints202603.1419.v1

18. ISO 5479:1997-05. Statistical interpretation of data - Tests for departure from the normal distribution. Available from: URL: https://www.iso.org/standard/22506.html [cited 2026 Jan 5].
19. Shapiro-Wilk Test Calculator. Statistics Kingdom; 2017. Available from: URL: https://www.statskingdom.com/shapiro-wilk-test-calculator.html.